Oxygen-vacancy-related low-frequency dielectric relaxation and electrical conduction in Bi:$SrTiO_3$

Chen Ang and Zhi Yu
Department of Physics, Department of Materials Science and Engineering, Zhejiang University, 310027 Hangzhou, People's Republic of China
and Materials Research Laboratory, The Pennsylvania State University, University Park, Pennsylvania 16802

L. E. Cross
Materials Research Laboratory, The Pennsylvania State University, University Park, Pennsylvania 16802
(Received 23 December 1999)

The temperature dependence of dielectric properties and electrical conduction of $(Sr_{1-1.5x}Bi_x)TiO_3$ $(0.0133 \leqslant x \leqslant 0.133)$ was measured from 10 to 800 K. Three sets of oxygen vacancies related dielectric peaks (peaks *A*, *B*, and *C*) were observed. These peaks could be greatly suppressed or eliminated by annealing the samples in an oxidizing atmosphere, and enhanced or recreated by annealing in a reducing atmosphere. The results show that the Maxwell-Wagner polarization is not the main mechanism, and the Skanavi's model also cannot be directly applied. A tentative explanation was suggested. Peak *A*, observed in the temperature range of 100–350 K with the activation energy for dielectric relaxation $E_{relaxA} = 0.32$–0.49 eV, is attributed to the coupling effect of the conduction electrons with the motion of the off-centered Bi and Ti ions; the conduction carriers in this temperature range are from the first ionization of oxygen vacancies (V_o). Peaks *B* and *C* are also discussed.

I. INTRODUCTION

Perovskite-type ABO_3 ionic oxides have attracted considerable attention due to their dielectric, ferroelectric, semiconducting, conducting, and superconducting behavior. The electrical properties of this type of material are closely related to its crystal structure and oxygen vacancies, which can be controlled by doping or annealing in different oxygen partial pressure conditions. The influence of oxygen vacancies on the conductivity of the ABO_3 ionic oxides has been confirmed by a number of observations.[1,2] For example, for $SrTiO_3$ (ST), the change in the concentration of the oxygen vacancy could lead to the change of the electron concentration and hence make the system change from insulator to semiconductor, and to metallic (and superconducting) behavior.[2] However, for the electrical polarization, although the role of oxygen vacancies has been reported in some ways, a detailed study has not been reported, and the important role of the oxygen vacancies has received insufficient attention.

ST is one of the perovskite compounds that is extensively studied both experimentally and theoretically. ST shows many interesting properties, including quantum paraelectric behavior,[3] a structural phase transition,[4,5] quantum ferroelectric behavior,[5,6] and superconductivity.[2] The behavior is related to the lattice vibration, electric polarization, and the transportation of electrons in the matrix of the ST lattice. In general, those studies were mainly carried out at low temperatures. On the other hand, the interesting low-frequency dielectric relaxation behavior was found in ST, especially, for the doped ST systems.[7–10] The dielectric anomalies with frequency dispersion were detected in the temperature range of 200–900 K, which are not related to the possible paraelectric-ferroelectric transition, but closely related to the oxygen vacancies.

For example, dielectric relaxation behavior has been studied for La-doped ST. Dielectric peaks with frequency dispersion at 170 and 470 K were reported early by Tien and Cross[7] and recently, another peak around 70 K by Iguchi and Lee.[8] Moreover a series of ST ceramics containing rare-earth ions were systematically studied by Johnson, Cross, and Hummel[9] and it was reported that the dielectric peaks occurred with the activation energy ranging from 0.20 to 0.45 eV for different rare-earth ions and various doping concentrations. The authors mainly adopted the Skanavi model to explain the physical mechanism of observed dielectric relaxation, i.e., the existence of *A* site vacancies in the perovskite ABO_3 lattice introduced by the lanthanum substitution distortion of the oxygen octahedron, producing more than one possible off-center site for the Ti^{4+} ion. The relaxation arose from the thermal motion over potential barriers separating these alternative sites.[9]

On the other hand, Stumpe *et al.*[10] reported that dielectric relaxation occurred in the temperature range 600–950 K for ST and 700–1100 K for $BaTiO_3$ (BT). They explained the results as the combined effect of bulk and surface properties, namely, Maxwell-Wagner polarization. Most recently, Maglione *et al.*[11] reported dielectric relaxation phenomena in a number of the perovskite materials containing titania, such as in $BaTiO_3$-, $CaTiO_3$-, and $PbTiO_3$-based systems. They found that the dielectric relaxation was closely related to the oxygen vacancies in the samples. The activation energy for dielectric relaxation is around 1.17–1.48 eV, and the activation energy of conduction is in the range of 1.07–1.31 eV, for $PbTiO_3$ doped with La. Maglione *et al.* attributed this phenomenon to a space-charge polarization in which the free

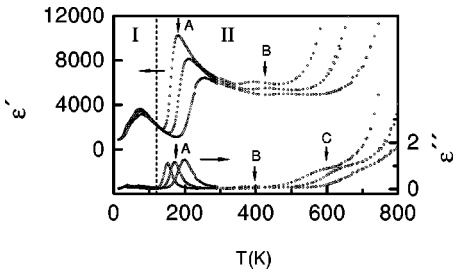

FIG. 1. Temperature dependence of ϵ' and ϵ'' of the as-sintered $(Sr_{1-1.5x}Bi_x)TiO_3$ sample with $x=0.0133$ at 100 Hz, 1 kHz, and 10 kHz (from top to bottom).

carriers are stored at the two dielectric electrode interfaces.

Obviously, this type of dielectric relaxation behavior is a common feature in the perovskite structure oxides containing titania.

The dielectric relaxation of Bi-doped ST solid solutions was first reported by Skanavi *et al.*[12] and Smolenskii *et al.*[13] By the systematic study of the dielectric properties of the solid solution $(Sr_{1-1.5x}Bi_x)TiO_3$ system, in a wide temperature range, some of the present authors[14] have recently reported that a ferroelectric relaxor behavior occurs in ST by introducing Bi ions. In addition, other sets of permittivity peaks with frequency dispersion were also observed.[15] For example, for $x=0.002$, the peaks around 22 K, 37 K, and 65 K (at 10 kHz) occurs, which are attributed to the defect modes.

In the present paper, besides the peaks mentioned above, we observed several dielectric relaxation peaks in Bi-doped ST, which are intimately related to the oxygen vacancies and electrons. The physical nature of the low-frequency dielectric relaxation peaks is discussed.

II. EXPERIMENTAL PROCEDURE

The ceramic samples were prepared by the solid-state reaction. Starting materials ($SrCO_3$, Bi_2O_3, and TiO_2) were weighed according to the composition $(Sr_{1-1.5x}Bi_x)TiO_3$, where $x=0.0133$, 0.0267, 0.04, 0.0533, 0.08, 0.10, and 0.133, respectively. The weighed batches were mixed, calcined, and pressed into disks. Finally, the samples were sintered from 1300 to 1380 °C for 2 h in air. Gold, silver, and gold/palladium electrodes were made for dielectric measurements. No dependence of dielectric behavior on electrodes was found.

The complex impedance of the samples was measured with an HP3330 LCZ Meter and a Solartron Impedance Gain-Phase Analyzer 1260 in the frequency range from 1 Hz to 1 MHz. The dc resistance of the samples was measured with a Keithley-617 Programmable Electrometer. The temperature dependence of dielectric and electric properties was measured in a cryogenic system from 11 to 300 K while the temperature of the samples was changing at a rate of 1 K/min. The measurements above room temperature were made by heating in a furnace from 300 to 800 K.

In order to compare the dielectric behavior, some samples were annealed in an oxidizing atmosphere (oxygen or air) or in a reducing atmosphere (nitrogen).

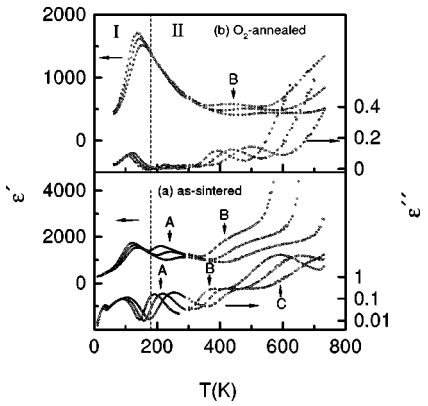

FIG. 2. Temperature dependence of ϵ' and ϵ'' of the $(Sr_{1-1.5x}Bi_x)TiO_3$ sample with $x=0.0533$, as-sintered (a), O_2 annealed (b) at 100 Hz, 1 kHz, and 10 kHz (from top to bottom).

III. RESULTS

A. Overall dielectric behavior and the influence of annealing

The temperature dependence of the real (ϵ') and imaginary parts (ϵ'') of the complex permittivity for the as-sintered samples with $x=0.0133$, 0.0533, and 0.10 is shown in Figs. 1–3, respectively. There are more than four sets of peaks occurring in the temperature range 10–800 K. In what follows, in order to describe the peaks conveniently, we denote region I and region II for temperatures as divided by the dashed line in Figs. 1–3, since the peaks in region I are not related to oxygen vacancies, however, the peaks in region II are closely related to oxygen vacancies (see the following). The permittivity peaks in region I were assigned as the ferroelectric relaxor peak.[13–15] In region II, there are three successive sets of peaks (more clearly seen for tan δ): the first set of permittivity peaks around 180–250 K (denoted as peak *A*), the second set around 300–350 K (denoted as peak *B*), and the third one around 550–680 K (denoted as peak *C*). With further increasing temperature (higher than 650 K), the peaks are covered by a rapid increase of ϵ and tan δ. With a careful inspection, we found that the permittivity maximum ϵ_{max} decreases with increasing Bi content for both peaks *A* and *B*. Peak *A* disappears for $x \geqslant 0.10$.

The temperature of the permittivity maximum (T_m) for peaks *A*, *B*, and *C* increases linearly with increasing Bi con-

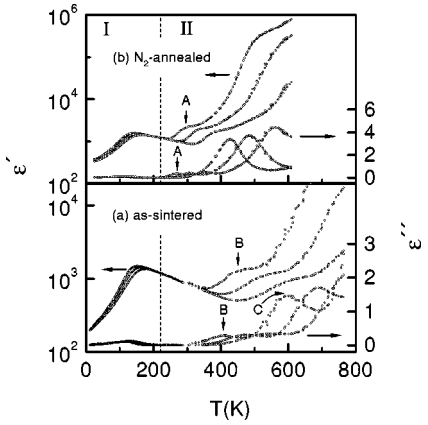

FIG. 3. Temperature dependence of ϵ' and ϵ'' of the $(Sr_{1-1.5x}Bi_x)TiO_3$ sample with $x=0.10$, as-sintered (a) and N_2 annealed (b) at 100 Hz, 1 kHz, and 10 kHz (from top to bottom).

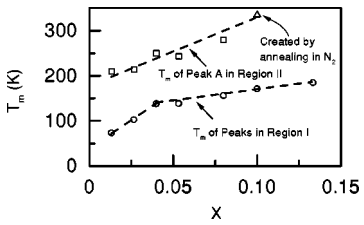

FIG. 4. Temperature of permittivity maximum of peak *A* in region II and ferroelectric relaxor peak in region I at 1 kHz versus Bi content for the as-sintered $(Sr_{1-1.5x}Bi_x)TiO_3$ ceramics, ($\triangle$) data from the sample with $x=0.1$ annealed in nitrogen.

tent, but at different rates. Figure 4 shows the compositional dependence of the T_m of peak *A*. For comparison, the T_m for the ferroelectric relaxor peaks versus the Bi content is also given.[14]

The as-sintered samples were annealed in oxidation atmospheres (oxygen or air). The dielectric behavior in region I is not significantly affected by annealing treatment in oxygen and in air. However, the dielectric behavior in region II is greatly influenced by annealing as shown in Fig. 2(b). The intensities of peaks *A*, *B*, and *C* were suppressed, in particular, peak *A* disappeared. For example, the annealing effect on peak *A* for $x=0.0133$ is shown in Fig. 5. It can be seen that with increasing annealing temperature and time in the oxidizing atmosphere, O_2 or air, peak *A* is gradually suppressed, and eventually disappears.

In order to inspect further the annealing effect, two as-sintered samples were annealed at 1000 °C for 88 h in the reduced atmosphere, nitrogen (N_2), one is for $x=0.0533$ with the presence of peak *A*, and another is for $x=0.10$ in which peak *A* is absent. After annealing in nitrogen, for $x=0.0533$, peak *A* is further increased and broadened. Interestingly, for $x=0.10$, peak *A* was created after annealing in nitrogen. The temperature dependence of permittivity for $x=0.1$ after annealing in N_2 at various frequencies is illustrated in Fig. 3(b). The T_m of the permittivity peak induced by annealing in N_2 for $x=0.1$, as shown in Fig. 4, also follows the variation tendency of the T_m of peak *A* with increasing Bi content.

Annealing in nitrogen increases the intensity of peaks *A*, *B*, and *C*, and in particular, it creates peak *A* for the sample with $x=0.1$, which has no peak *A* before annealing in N_2, evidencing that all sets of peaks are closely related to the oxygen vacancies.

Here it should be pointed out that the grain size is the same before and after annealing either in oxygen or nitrogen, within experimental errors.

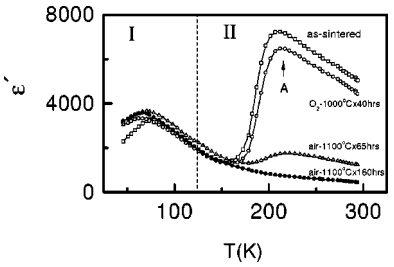

FIG. 5. Temperature dependence of ϵ' under different annealing conditions (atmosphere, temperature, and time) at 1 kHz for $(Sr_{1-1.5x}Bi_x)TiO_3$ ceramic with $x=0.0133$.

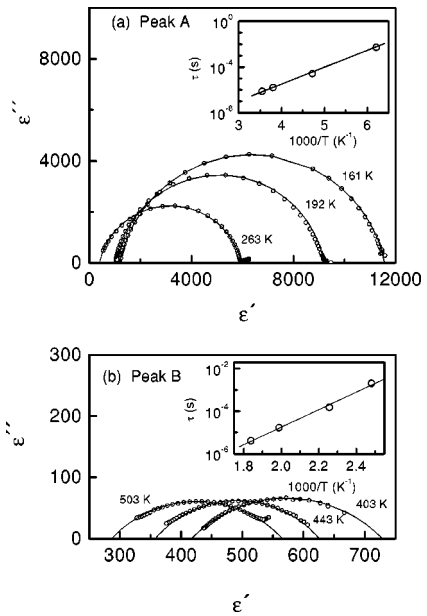

FIG. 6. Cole-Cole plot (ϵ'' vs ϵ') of the as-sintered $(Sr_{1-1.5x}Bi_x)TiO_3$ ceramics, (a) in the temperature range where peak *A* occurred for $x=0.0133$, (b) in the temperature range where peak *B* occurred for $x=0.0533$. Inset is relaxation time τ versus $1/T$. (Open circles: experimental data; circular arcs and lines: fitting curves.)

B. Dielectric relaxation behavior and electrical conductivity

1. Dielectric relaxation time and activation energy

We choose the samples with $x=0.0133$ and $x=0.0533$ to plot the curve of ϵ'' versus ϵ', i.e., the Cole-Cole plot for peaks *A* and *B*, respectively. As shown in Figs. 6(a) and 6(b), the data points fit well into a semicircular arc with the center lying underneath the abscissa, deviated from the ideal Debye model to some extent. Hence the modified Debye equation is adopted to evaluate the dielectric relaxation. The complex permittivity can be empirically described by the Cole-Cole equation:[16]

$$\epsilon^* = \epsilon_\infty + (\epsilon_0 - \epsilon_\infty)/[1+(i\omega\tau)^{1-\alpha}], \tag{1}$$

where ϵ_0 is the static permittivity, ϵ_∞ is the permittivity at high frequency, ω is the angular frequency, τ is the mean relaxation time, and $\beta=1-\alpha$, where α is the angle of the semicircular arc.

The ϵ' and ϵ'' can be rewritten from Eq. (1) in the following way:

$$\epsilon' = \epsilon_\infty + (\triangle\epsilon/2)\{1-\sinh(\beta z)/[\cosh(\beta z)+\cos(\beta\pi/2)]\}, \tag{2}$$

$$\epsilon'' = (\triangle\epsilon/2)\sin(\beta\pi/2)/[\cosh(\beta z)+\cos(\beta\pi/2)], \tag{3}$$

where $z=\ln(\omega\tau)$ and $\triangle\epsilon=\epsilon_0-\epsilon_\infty$. By fitting the experimental data to Eqs. (1)–(3), we can obtain the parameters, ϵ_0, ϵ_∞, β, and τ as a function of temperature. The obtained τ is plotted as a function of inverse temperature in the inset of Fig. 6. It is found that the τ follows the Arrhenius law,

$$\tau = \tau_0 \exp[E_{relax}/(k_B T)], \tag{4}$$

TABLE I. The activation energy of dielectric relaxation $E_{\text{relax}A}$, the temperature range ΔT_A in which peak A occurs, and the activation energy of electrical conduction $E_{\text{cond}A}$ in the ΔT_A, for $(Sr_{1-1.5x}Bi_x)TiO_3$ samples.

X	0.0133 (as-sintered)	0.0267 (as-sintered)	0.04 (as-sintered)	0.0533 (as-sintered)	0.0533 (N_2-annealed)	0.08 (as-sintered)
$E_{\text{relax}A}$ (eV)	0.32	0.31	0.43	0.48	0.48	0.49
ΔT_A (K)	130–310	140–320	150–330	170–350	170–350	200-380
$E_{\text{cond}A}$ (eV)	0.13			0.26	0.28	

where τ_0 is the relaxation time at infinite temperature, E_{relax} is the activation energy for relaxation, k_B is the Boltzmann constant, and T is the temperature. For peak B of the sample with $x=0.053$, $E_{relaxB}=0.48$ eV. The obtained τ versus $1/T$ follows the Arrhenius law for all the samples, the activation energies E_{relax} and the pre-exponential factor τ_0 are obtained by fitting the experimental data to Eq. (4) for peaks A, B, and C. The τ_0 for the three peaks is in the range of $(0.5–7)\times10^{-12}$ s, and the other parameters are summarized in Tables I, II, and III. It can be seen that E_{relaxA} is 0.32–0.48 eV, and E_{relaxB} is 0.74–0.89 eV for the as-sintered samples. Both E_{relaxA} and E_{relaxB} slightly increase with increasing Bi content. No influence of annealing in oxidation atmosphere on E_{relaxA} and E_{relaxB} was found, however, after annealing in nitrogen N_2, E_{relaxB} decreases to ~0.64 eV.

2. dc electrical conductivity and its activation energy

The temperature dependence of the dc conductivity (σ_{dc}) of the samples with $x=0.0533$ and 0.1, both as-sintered and annealed in nitrogen, is plotted in Fig. 7. The conductivity can be expressed by the following equation:

$$\sigma=\sigma_0\exp[E_{cond}/(k_BT)], \tag{5}$$

where σ_0 is the pre-exponential term and E_{cond} is the conduction activation energy. The values of E_{cond} obtained for the samples are summarized in Tables I, II, and III.

Comparing the conduction data with the dielectric data, three points should be emphasized.

(i) It is interesting to note that the temperature region for the different slopes of the conductivity against $1/T$ (corresponding to the different types of conduction mechanisms), coincides with the temperature region where the different sets of permittivity peaks occur. This indicates that there is a close relation between dielectric behavior and conduction behavior for peaks A, B, and C.

(ii) In the temperature range 200–350 K where peak A occurs, for $x=0.0533$, E_{condA} is 0.26 and 0.28 eV for the as-sintered and nitrogen-annealed samples, respectively (shown in Table I). The similar values imply that the conduction mechanism does not change after annealing in N_2.

(iii) However, in the temperature range 350–600 K where peak B occurs, after annealing in N_2, for $x=0.0533$ and 0.10, E_{condB} decreases and simultaneously E_{relaxB} decreases as shown in Table II. Interestingly, we notice that E_{condB} and E_{relaxB} show almost the same values, ~0.64 eV, for both samples after annealing in N_2.

Points (ii) and (iii) indicate that the dielectric and conduction mechanisms of peak A are not changed, but peak B is changed by annealing in N_2. This will be discussed in detail in Sec. IV C again.

3. Optical spectra

The optical absorption was measured for the Bi-doped ST samples. Figure 8 shows the optical spectra of the as-sintered samples with $x=0.0267$ and 0.133 and the sample for $x=0.0267$ annealed in an oxidizing atmosphere. The band gap of $E_g=\sim3.3$ eV was obtained. It is noticed that there is a broad peak at ~1.3 eV for the as-sintered samples with low-Bi concentration doping. However, this absorption peak has not been observed for the sample doped with high-Bi concentration ($x=0.133$) or the samples ($x=0.0267$) annealed in the oxidizing atmosphere.

C. Summary of results

The above results indicated that several sets of permittivity peaks occur in the temperature range 10–800 K. In region I, the permittivity peaks were already discussed and attributed to ferroelectric relaxor[13,14] and defect modes.[15] In this paper, we discuss the dielectric behavior in region II.

(i) Both peaks A and B are present for lower-Bi concentration, while peak A disappears at higher concentration of $x\geqslant0.10$.

(ii) Peaks A could be gradually decreased and eventually eliminated by annealing in oxidation atmospheres. Peak B is

TABLE II. The activation energy of dielectric relaxation $E_{\text{relax}B}$, the temperature range ΔT_B in which peak B occurs, and the activation energy of electrical conduction $E_{\text{cond}B}$ in the ΔT_B, for $(Sr_{1-1.5x}Bi_x)TiO_3$ samples.

X	0.0267 (as-sintered)	0.04 (as-sintered)	0.0533 (as-sintered)	0.0533 (annealed in O_2)	0.0533 (annealed in N_2)	0.10 (as-sintered)	0.10 (annealed in N_2
$E_{\text{relax}B}$ (eV)	0.74	0.77	0.82	0.76	0.64	0.86	0.64
ΔT_B (K)	350–460	360–470	350–510	350–500	350–600	350–600	350–650
$E_{\text{cond}B}$ (eV)	0.59	0.68	0.76		0.63	0.78	0.66

TABLE III. The activation energy of the dielectric relaxation $E_{\mathrm{relax}C}$, the temperature range ΔT_C in which peak C occurs for $(Sr_{1-1.5x}Bi_x)TiO_3$ as-sintered samples.

X	0.0133	0.0267	0.0533	0.08	0.10	0.133
$E_{\mathrm{relax}C}$ (eV)	1.12	1.05	1.09	1.05	1.09	0.99
ΔT_C (K)	500–750	500–750	500–750	500–750	550–770	560–800

greatly decreased and expected to be eliminated by further annealing in an oxidization atmosphere as observed in La:ST.[17] These peaks could be enhanced or created by annealing in a reducing atmosphere.

(iii) With increasing Bi content, both T_{mA} and T_{mB} increase and the activation energies E_{relaxA} and E_{relaxB} rise simultaneously.

(iv) The permittivity maximum decreases with the increasing Bi content for both peaks *A* and *B*.

(v) Peak *C* was observed in the temperature range 550–800 K for all the samples. With increasing Bi content, the temperature of the peak maximum (T_{mC}) increases.

(vi) The activation energy E_{relaxC} of the dielectric relaxation is in the range 0.99 to 1.12 eV.

(vii) The activation energy E_{condC} of the electrical conduction in the temperature range where the permittivity peak *C* occurs is 1.02–1.13 eV.

IV. DISCUSSION

A. Review of the previous models

Based on the experimental facts above, a basic question is: ''What is the physical nature of the dielectric peaks with frequency dispersion?'' or ''What are the polarization species?'' As mentioned in the introduction, similar dielectric relaxation behavior in pure ST, BT, or La-doped ST was mostly attributed to two possibilities, one is the so-called Maxwell-Wagner polarization (i.e., the interfacial polarization); another is attributed to the thermally activated Ti^{4+} ion hopping according to the Skanavi's model.[12]

1. Maxwell-Wagner-type polarization

The Maxwell-Wagner effect, or interfacial phenomena model[18] was usually adopted to explain the dielectric relaxation with extremely high permittivity. The common interpretation consists of assuming a whole series of barrier phenomena, or even a complete series-parallel array of barrier-volume effects, such as might arise if the material consisted of grains separated by more insulating intergrain barriers. This kind of heterogeneous medium effect is described under the Maxwell-Wagner model.[18] The superficial point of this model is that it can be developed into a whole distribution of interfacial effects, and it has an apparent plausibility to providing any expected distributions of Debye-like relaxation times. The main disadvantage is that it cannot be proved.[19]

The dielectric anomaly around 900 K in ST was explained as a result of a group of series and parallel arrays of Schottkey barriers.[10] Although a calculation according to this hypothesis was in agreement with the experimental data observed, it is not convincing to have deep inspect into its physical picture. Indeed, from the equivalent circuit, the expected numerical fitting can be always obtained. However, it is difficult to suppose that, in a physical sense, the species corresponding to the equivalent circuit does exist in the material.

As argued by Jonscher,[19] the Maxwell-Wagner model cannot explain why a seldom distribution of relaxation time of Maxwell-Wagner effect can give a systematic dependence of the relaxation parameters on the ionic size of rare-earth concentrations or on the Bi concentration in Bi-doped ST.

In addition, in terms of the Maxwell-Wagner model, it is very difficult to explain dielectric relaxation behavior appearing in the same temperature region for the single crystals and polycrystalline ceramics, in which the structural heterogeneity is certainly different in both cases.

In the present paper, the high value of the permittivity of peak *A* (for $x=0.0133$, at 161 K and 1 kHz, $\Delta\epsilon=\sim 10\,400$) as well as the conductivity values could suggest an interfacial polarization of the Maxwell-Wagner type.[18] This type of interfacial polarization was usually adopted to explain the experimental results in ST-based materials used as boundary layer capacitors, with extremely high

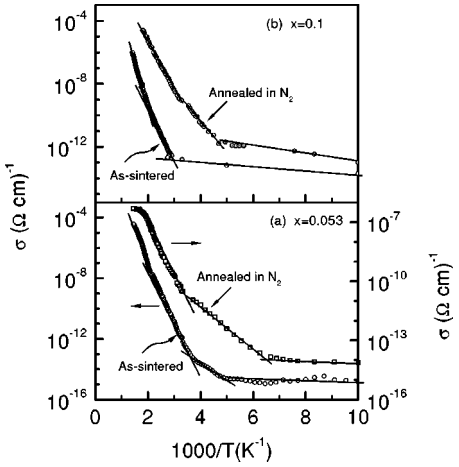

FIG. 7. Temperature dependence of dc conductivity (σ_{dc}) of $(Sr_{1-1.5x}Bi_x)TiO_3$ sample, (a) $x=0.0533$ and (b) $x=0.1$, for both as-sintered and annealed in N_2.

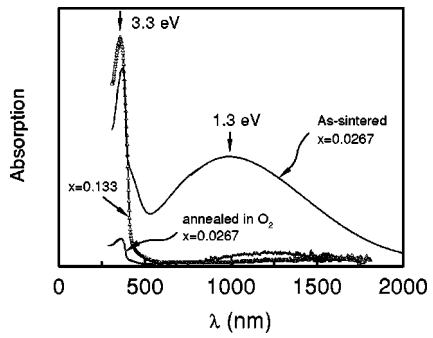

FIG. 8. Absorption spectra of the as-sintered samples with $x=0.0267$, 0.133, and the sample with $x=0.0267$ after annealing in the oxidizing atmosphere.

permittivity.[20] Interfacial polarization could take place due to the existence of two different conducting areas if the monophasic samples have an inhomogeneous microstructure. This type of microstructure could be originated by the loss of oxygen from the bulk of the grains during the high-temperature sintering followed by a re-oxidation of a surface layer at the grain boundaries during the cooling-down process. A microstructure consisting of high-conductive grains and low-conductive grain boundaries was then formed and interfacial polarization occurred.

If this was so, the presence of peak *A* in the as-sintered samples, and the disappearance of these peaks after annealing in O_2 could then be explained. However, it is difficult to explain why higher peaks with the same activation energy for relaxation were obtained after the sample was annealed in N_2 at 1000 °C for 88 h, since when the samples were annealed in N_2, reduction on the surface layer, which was previously oxidized during the sintering-cooling process, would happen. It is therefore unlikely that the interfacial polarization is the origin of peaks *A*, *B*, and *C*.

It should be mentioned that before and after annealing both the lattice parameter and the grain size are the same within the experimental error and a homogeneous distribution of the elements (Sr, Bi, and Ti) was observed by the scanning electron microscope x-ray line profile analysis. This strongly supports that these peaks cannot be attributed to the interfacial polarization.

Moreover, it is doubtful that the Maxwell-Wagner model can provide a systematic dependence of the polarization and relaxation parameters on the Bi concentration.

The simplest form of interfacial effect is represented by a capacitive layer arising near an electrode as a result of the formation of a Schottkey barrier which is less conducting than the bulk of the sample. This is the so-called space-charge model. Recently the space-charge model was adopted to explain dielectric relaxation occurring in a number of perovskite oxides in the temperature range 600 to 800 K by Bidault *et al.*[11] They suggested that free charges bounded to interfaces of grain boundaries or crystal surfaces contributed to dielectric polarization and the activation energy for relaxation was the same with those of electrical conduction.

This model was also used by Blanc and Staebler[21] to explain the conduction behavior in ST doped with transition metals under electrocoloration. Although this model can overcome the difficulty of single crystals and polycrystalline ceramics, it still cannot explain *the several peaks* successively occurring in doped ST.

In addition, the possibility of the contact between the electrodes and samples influencing the dielectric properties can be excluded, because the dielectric behavior is independent of the thickness of the samples (0.5 and 1 mm) as well as of the type of the electrodes (Au, Ag, and Au/Pd) adopted for Bi-doped ST.

2. Skanavi model

Skanavi's model described the small motion of Ti^{4+} in six equivalent potential minima, which caused the reorientation of the dipoles, and contributed to the dielectric relaxation. The model suggested that a very strong internal field will be induced because of a proper crystal structure of perovskite ABO_3, similar to that of BT, and a small motion of the Ti^{4+} ions will give a very high permittivity.[12] In the Skanavi model, the polarization species are Ti^{4+} ions. In the present paper, the experimental facts strongly evidence that the dielectric relaxation is closely related to the oxygen vacancies. Our recent work has shown that the dielectric peaks with frequency dispersion in La-doped ST can be absolutely eliminated by prolonging annealing time in an oxidation atmosphere,[17] which does not support the previous explanation in terms of Skanavi's model.[7–9] The experimental facts are that all the peaks for La-doped ST and the three peaks (*A*, *B*, and *C*) for Bi-doped ST in this paper are related to the oxygen vacancies.[22] From this point of view, Skanavi's model, at least, cannot be directly adopted to explain the present paper.

B. Defect structure

From the experimental results in the present paper and the review of the related models mentioned above, the possibility of the Maxwell-Wagner-type interfacial polarization can be excluded, at least it is not the main mechanism. However, the experimental results indicate that the dielectric peaks are closely related to the redox process, hence, it is very possible that the dielectric peaks are related to the oxygen vacancies existing in the samples. In the following section, we first discuss the defect structure in Bi-doped ST, before considering possible physical mechanism.

Previous work[20] indicated that in donor-doped ST, as the donor concentration is greater than 0.2 at. %, the cation vacancy compensation is predominant (and the electron compensation can be neglected). In the present paper, the Bi concentration x for the $(Sr_{1-1.5x}Bi_x)TiO_3$ solid solution is in the range of 1.33–13.3 at. %, which is much higher than the 0.2 at. %. In fact, based on consideration of the charge balance, Sr sites vacancies were induced, which are assumed to compensate the heterovalent substitution of the Bi^{3+} ions for Sr^{2+} ions. From this point of view, for $(Sr_{1-1.5x}Bi_x)TiO_3$ ($x=1.33\%-13.3\%$) or written as $[Sr_{1-1.5x}Bi_x(V_{Sr})_{0.5x}]TiO_3$ (V_{Sr} is Sr vacancy), the electrical unbalance caused by the trivalent Bi ion substitution for the divalent Sr ions is compensated by the creation of strontium vacancies, i.e.,

$$Bi_2O_3 \Leftrightarrow 2Bi_{Sr}^{\cdot} + 3O_o^{\times} + V_{Sr}'', \tag{6}$$

where the Kröger–Vink notation of defects is adopted (the notation is also used in follows). V_{Sr}'' represents the strontium vacancy carrying two excess negative charges.

The experimental results show that several relaxation processes appear in the $(Sr_{1-1.5x}Bi_x)TiO_3$, which can be eliminated by annealing in the oxidizing atmosphere, and re-created or enhanced by annealing in the reducing atmosphere. These phenomena strongly suggest that the relaxation processes are related to oxygen vacancies (as well as electrons).

However, what mechanism causes oxygen vacancy? In the earlier literature, Skanavi *et al.*,[12] and Burn and Neirman[20] pointed out that, although the trivalent Bi could be mainly compensated by strontium vacancies as indicated as Eq. (6), oxygen vacancies could be easily created by loss of oxygen from the crystal lattice at low oxygen partial pres-

sure or during sintering at high temperatures ($T_s \geqslant 1350\,^{\circ}\mathrm{C}$) for Bi-doped ST,[23–27] according to

$$O_o \Leftrightarrow V_o + 1/2\ O_2. \tag{7}$$

The lower the Bi concentration, the higher the sintering temperature. The higher V_o concentration for lower Bi concentration samples and lower V_o concentration for higher Bi concentration samples are expected. In the present paper, for the as-sintered samples doped with low Bi concentration, the oxygen vacancies appear. Annealing in N_2 increases greatly the V_o concentration, while annealing in O_2 eliminates the V_o.

It is well known that in the perovskite structure materials containing titanate, the ionization of the oxygen vacancy will create the conducting electrons, rewritten as

$$V_o \Leftrightarrow V_o^{\cdot} + e', \tag{8a}$$

$$V_o^{\cdot} \Leftrightarrow V_o^{\cdot\cdot} + e', \tag{8b}$$

or these electrons might be bonded to Ti^{4+} in the form of

$$Ti^{4+} + e' \Leftrightarrow Ti^{3+}. \tag{9}$$

However, as indicated by Ihrig and Hennings,[28] it is difficult to determine whether the weakly bonded electrons are located near V_o or near Ti ions. The exact location of the electrons depends on the details of structure, temperature range, etc. It was, however, shown that the oxygen vacancies lead to shallow level electrons. These electrons may be trapped by Ti^{4+} ions or oxygen vacancies, forming color centers. These electrons are easy to be thermally activated becoming conducting electrons. In fact, the samples doped with low-Bi concentration show dark-gray color, peaks *A*, *B*, and *C* occur in these samples, and simultaneously, the broad optical absorption peak around ~ 1.3 eV was observed. After annealing in an oxidizing atmosphere, peak *A* disappears, peak *B* was greatly suppressed or eliminated, the optical absorption peak at ~ 1.3 eV was also greatly suppressed, the samples show bright-yellow color, and the resistivity is enhanced by 1–2 orders of magnitude. This confirms that there is close correlation among the oxygen vacancies, electrons, color centers, and the dielectric relaxation.

C. Explanations

1. Peak A: Dielectric relaxation in the temperature range 100–350 K

In this paper, the activation energy for the conduction in the temperature range 100–350 K is between 0.13 and 0.28 eV, which is near the activation energy, 0.1 eV, of the first-ionization of oxygen vacancies (V_o) as described in Eq. (8a).[29] This indicates that in this temperature range, the free conduction electrons result from the first-ionization of oxygen vacancies.

In addition, the contribution of the conduction electrons (or holes or protons) to dielectric polarization has been reported in many systems for both single crystals and polycrystalline ceramics.[30–34] In order to explain the very high permittivity in Nb-doped BT, Maglione and Belkaoumi[34] suggested an *electron relaxation–mode coupling* model, i.e., the polarization was greatly enhanced by the interaction of the electrons (created by the ionization of oxygen vacancies) and the dielectric relaxation process. In this case, even with low concentration of the dipoles, the system could exhibit a very high permittivity.

The experimental facts show that peak *A* occurs at the high-temperature side of the ferroelectric relaxor peak (see Figs. 1–3). It is known that for a ferroelectric relaxor, like PMN and PLZT, microdomains are observed at higher temperatures far from the temperature of the ferroelectric relaxor peak.[35] It is reasonable to assume that microdomains may exist in Bi-doped ST at the high-temperature side of the ferroelectric relaxor peak, i.e., in the temperature range where peak *A* is observed. The observed activation energy of the dielectric relaxation for peak *A* is between 0.32 and 0.49 eV.

In the present paper, the authors suggest that peak *A* results from the contribution of the combination effect of the reorientation of the off-center Bi and Ti ions coupling with the conducting electrons. That is, in the as-sintered samples doped with low-concentration Bi ions, the conducting electrons appear due to the ionization of the oxygen vacancies; these electrons interact with the dipoles of the off-center Bi and Ti ions (these dipoles may also form the microdomains existing at the high temperature side of the ferroelectric relaxor peak), and contributes to the high-dielectric relaxation step for peak *A*.

Based on this hypothesis, the experimental fact (i) can be explained, i.e., when the Bi content $x \leqslant 0.08$, the defect structure can be described by Eqs. (6)–(8). The permittivity of the material depends on the concentration of the electrons and their interaction with the dipoles of off-center Bi and Ti ions. Because of the higher sintering temperature used when the Bi concentration is low, higher concentration of intrinsic oxygen vacancies, and hence higher concentration of the electrons [described by Eq. (8)] are achieved. This results in the high permittivity step in the materials. As the Bi concentration $x \geqslant 0.10$, the sintering temperature for the samples is relatively lower [the defect structure of the sample is mainly described by Eq. (6)], the concentration of both oxygen vacancies and electrons is small, and hence, peak *A* disappeared.

The oxygen vacancies can be filled after heat treatment in an oxidizing atmosphere, and will be again created after annealing in N_2, hence the concentration of the electrons varies. This provides an explanation for the variation of peak *A* described by the experimental fact (ii).

The experimental fact (iii) can be rationalized since with the increase in the substitution of the Bi ions, the crystal lattice will be much distorted;[12] then it is reasonable to assume that the movement of the dipoles becomes difficult, and higher activation energy for the dielectric relaxation is needed.

2. Peak B: Dielectric relaxation in the temperature range 350–600 K

1. *Samples* ($x = 0.0533$ *and 0.1) annealed in* N_2. For the samples annealed in N_2, the concentration of oxygen vacancies and electrons can be greatly increased. The activation energies of dielectric relaxation and dc electrical conduction are in the range ~ 0.63–0.66 eV for both samples with x

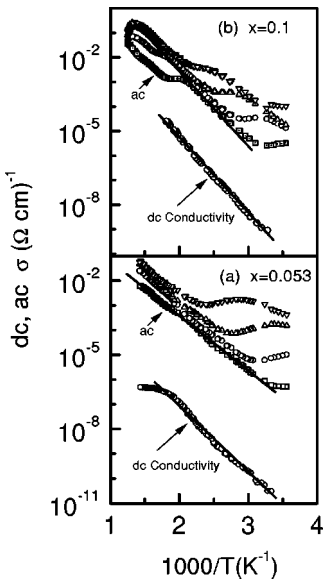

FIG. 9. Temperature dependence of the ac and dc conductivity of peak B in $(Sr_{1-1.5x}Bi_x)TiO_3$ sample annealed in N_2; (a) $x=0.0533$, (b) $x=0.1$. ac conductivity: ▽, 100 Hz; △, 1 kHz; ○, 10 kHz; □, 100 kHz.

$=0.0533$ and 0.1. The typical behavior of σ_{ac} and σ_{dc} vs $1/T$ is shown in Figs. 9(a) and 9(b), the similar activation energies for dielectric relaxation and dc conduction suggest the same physical nature for both conduction and dielectric relaxation. The dielectric relaxation seems, therefore in this case, to be related to the trap-controlled ac conduction.

For Eq. (8b), Long and Blumenthal reported that the second-ionization energy $V_o^{\cdot}$ is around $E_d=1.4$ eV.[36] Since the energy gap of ST is $E_g=3.3$ eV, the energy level E_d of $V_o^{\cdot}$ is located near the middle of the band gap. In the temperature range 350–600 K, if the electrical conduction is governed by the thermal excitation of carriers from the second ionization of oxygen vacancies ($V_o^{\cdot}$) to the conduction band, one could obtain an activation energy around 0.7 eV ($E_d/2$) for conduction.

The observed activation energy for the conduction, $E_{cond}=0.63$–0.66 eV, is very near 0.7 eV ($E_d/2$) (in fact, in this paper, the $E_d=1.3$ eV, see below), this indicates that the conduction carriers are electrons from the second ionization of oxygen vacancies ($V_o^{\cdot}$). Hence, it is reasonable to assume that the hopping of the electrons contributes to the dielectric relaxation in the samples annealed in N_2, whose physical mechanism is similar to the polaron behavior observed in some oxides;[31–33] and the long-distance movement of the electrons contributes to the conduction.

2. *As-sintered samples.* For the Bi concentrations $x=0.0267$, 0.04, 0.0533, and 0.10, the activation energies for conduction lie in the range 0.59–0.78 eV, while the activation energies for the dielectric relaxation lie in the range 0.74–0.86 eV in the temperature range 350–600 K.

In the optical absorption spectra for pure ST, and Nb-, Ni-, and Fe-doped ST, Wild *et al.*[37] reported a broad peak at $\sim$1.6 eV, which is independent of the type and concentration of impurities. This peak was considered due to an intrinsic mechanism, namely, the host-crystal peak, and was attributed to the energy level associated with two electrons trapped at an oxygen vacancy ($V_o^{\cdot\cdot}$).[37] In this paper, we observed that a peak at $\sim$1.3 eV in the optical-absorption spectra for the as-sintered samples doped with low-Bi concentration. This value is a little bit lower than the results of Wild *et al.*,[37] however, it is in good agreement with the second-ionization energy, $E_d=1.4$ eV, of oxygen vacancies reported by Long and Blumenthal.[36] The disappearance of the optical-absorption peak at $\sim$1.3 eV for the samples annealed in the oxidizing atmosphere and the samples with high-Bi concentration doping ($x=0.133$) indicated that the $V_o^{\cdot}$ were greatly suppressed for those samples. Correspondingly, the dielectric behavior shows that peak B was greatly suppressed by annealing in the oxidizing atmosphere or for high-Bi concentration doping. From this, it can be concluded that the peak B is related to the $V_o^{\cdot}$. In addition, due to the fact that the activation energy for conduction is always smaller than the dielectric relaxation activation energy for the samples in the temperature range where peak B is observed, it suggests that the polarization is of the dipole type. The dielectric relaxation could therefore be tentatively attributed to motion of the dipoles, very probably the defect associate ($V''_{Sr}-V_o^{\cdot}$), under the external field.

The experimental values of conduction activation energy, $E_{cond}=0.59$–0.78 eV, are not far from the expected conduction activation energy of 0.7 eV ($E_d/2$). The small deviation from the value of 0.7 eV may be due to the distortion of the ST lattice with the increasing concentration of the dopant. Hence, it is reasonable to assume that in this temperature range, the conduction carriers are also from the second-ionization of oxygen vacancies, the same as those for samples annealed in N_2.

Obviously, annealing in O_2 will decrease the concentration of oxygen vacancies favoring the decrease in the concentration of defect pairs and the concomitant decrease in the peak intensities. On the contrary, the annealing in N_2 will favor the increase in the concentration of oxygen vacancies and the variation in peak intensity in the opposite way.

3. Peak C: Dielectric relaxation in the temperature range 500–800 K

In the temperature range of 500–800 K, it was reported by Waser[38] that the oxygen vacancies can move due to thermal activation. Waser reported that at 513 K, the oxygen vacancy mobility is from 3×10^{-9} to 7×10^{-9} cm^2/(V s), and the activation energy of oxygen vacancy is 1.005–1.093 eV.[38] In addition, it was also reported by Paladino[25] that the activation energy for diffusion of the doubly-ionized oxygen vacancies in ST crystal is 0.98 eV. This is in good agreement with the experimental results of the activation energy (0.99–1.12 eV) obtained from the dielectric relaxation in the present paper. So the dielectric relaxation occurring in the temperature range 500–800 K for $(Sr_{1-1.5x}Bi_x)TiO_3$ samples could be related to the movement of the doubly-ionized oxygen vacancies under the external ac electric field.

On the other hand, the activation energy for conduction is about 1.02–1.13 eV in this paper, this is also in agreement with the results reported by Waser[38] and Paladino,[25] and it could be concluded that the conducting species are also the doubly-ionized oxygen vacancies.

Based on the results mentioned above, we suggested that, in the temperature range of 500–800 K, the doubly-ionized

oxygen vacancies act as ''polarons.'' The short-range hopping of oxygen vacancies, similar to the reorientation of the dipole, leads to a dielectric relaxation, peak *C*. The long-range motion of the doubly-ionized oxygen vacancies leads to dc electrical conduction.

V. CONCLUSION

The temperature dependence of dielectric properties of $(Sr_{1-1.5x}Bi_x)TiO_3$ solid solutions was measured in the temperature range of 10–800 K, and the influence of annealing at different atmospheres on the dielectric properties was studied. The results show that three sets of dielectric peaks (peaks *A*, *B*, and *C*) are related to oxygen vacancies. The three peaks could be greatly suppressed or eliminated by annealing the samples in the oxidizing atmosphere, and enhanced or recreated by annealing in the reducing atmosphere.

The discussion of the polarization and conduction mechanism shows that the Maxwell-Wagner polarization is not the main mechanism, and the Skanavi model cannot be directly applied to the present paper. The tentative explanation was suggested.

(i) Peak *A* (observed in the range ~100–350 K, $E_{relaxA}=0.32$–0.49 eV) is attributed to the coupling effect of the conduction electrons with the motion of the off-center Bi and Ti ions; in this temperature range, the carriers for electrical conduction result from the first-ionization of oxygen vacancies (V_o).

(ii) Peak *B* (observed in the range ~350–650 K) for the samples annealed in N_2 with $E_{relaxB}=0.63$–0.66 eV is attributed to the trap-controlled ac conduction around doubly ionized oxygen vacancies $V_o^{\cdot\cdot}$; the activation energy for dc electrical conduction ($E_{condB}=0.63$–0.66 eV) indicates that the conduction carriers are from the second ionization of oxygen vacancies. For the as-sintered samples, Peak *B*, with $E_{relaxB}=0.74$–0.86 eV, is attributed to the motion of the defect associate $(V''_{Sr}-V_o^{\cdot\cdot})$. The electrical conduction ($E_{condB}=0.59$–0.78 eV) is due to the motion of the electrons from the second ionization of oxygen vacancies, the same as those in the samples annealed in N_2.

(iii) Peak *C* (observed in the range ~600–800 K) with $E_{relaxC}=0.99$–1.12 eV is attributed to the short-range motion of the $V_o^{\cdot\cdot}$; and the long-range motion of the $V_o^{\cdot\cdot}$ leads to dc electrical conduction.

[1] *Physical Properties of High Temperature Superconductors, I and II*, edited by D. M. Ginsberg (World Scientific, Singapore, 1989).
[2] J. E. Schooley, W. R. Hosler, and M. L. Cohen, Phys. Rev. Lett. **12**, 474 (1964).
[3] K. A. Müller and H. Burkhard, Phys. Rev. B **19**, 3593 (1979).
[4] F. W. Lytle, J. Appl. Phys. **35**, 2212 (1964).
[5] K. A. Müller and W. Berlinger, Phys. Rev. Lett. **26**, 13 (1974).
[6] J. G. Bednorz and K. A. Müller, Phys. Rev. Lett. **52**, 2289 (1984).
[7] T. Y. Tien and L. E. Cross, Jpn. J. Appl. Phys. **6**, 459 (1967).
[8] E. Iguchi and K. J. Lee, J. Mater. Sci. **28**, 5809 (1993).
[9] D. W. Johnson, L. E. Cross, and F. A. Hummel, J. Appl. Phys. **41**, 2828 (1970).
[10] R. Stumpe, D. Wagner, and D. Bauerle, Phys. Status Solidi A **75**, 143 (1983).
[11] O. Bidault, P. Goux, M. Kchikech, M. Belkaoumi, and M. Maglione, Phys. Rev. B **49**, 7868 (1994).
[12] G. I. Skanavi and E. N. Matveeva, Zh. Éksp. Teor. Fiz. **30**, 1047 (1956) [Sov. Phys. JETP **3**, 905 (1957)]; G. I. Skanavi, I. M. Ksendzov, V. A. Trigubenko, and V. G. Prokhvatilov, *ibid.* **33**, 320 (1957) [**6**, 250 (1958)].
[13] G. A. Smolenskii, V. A. Isupov, A. I. Agranovskaya, and S. N. Popov, Fiz. Tverd. Tela (Leningrad) **2**, 2906 (1963) [Sov. Phys. Solid State **2**, 2584 (1961)].
[14] Chen Ang, Zhi Yu, P. M. Vilarinho, and J. L. Baptista, Phys. Rev. B **57**, 7403 (1998).
[15] Chen Ang, J. F. Scott, Zhi Yu, H. Ledbetter, and J. L. Baptista, Phys. Rev. B **59**, 6661 (1999); Chen Ang, Zhi Yu, J. Hemberger, P. Lunkhemer, and A. Loidl, *ibid.* **59**, 6665 (1999); Chen Ang, Zhi Yu, P. Lunkhemer, J. Hemberger, and A. Loidl, *ibid.* **59**, 6670 (1999).
[16] K. S. Cole and R. H. Cole, J. Chem. Phys. **9**, 341 (1941).
[17] Zhi Yu, Chen Ang, and L. E. Cross, Appl. Phys. Lett. **74**, 3044 (1999).
[18] A. von Hippel, *Dielectric and Waves* (Wiley, New York, 1954).
[19] A. K. Jonscher, *Dielectric Relaxation in Solids* (Chelsea Dielectrics, London, 1983), Chap. 8.
[20] I. Burn and S. Neirman, J. Mater. Sci. **17**, 3510 (1982).
[21] J. Blanc and D. L. Staebler, Phys. Rev. B **4**, 3548 (1971).
[22] Zhi Yu, Chen Ang, P. M. Vilarinho, P. O. Mantas, and J. L. Baptista, J. Eur. Ceram. Soc. **18**, 1621 (1998); **18**, 1629 (1998).
[23] N. H. Chan, R. K. Sharma, and D. M. Smyth, J. Electrochem. Soc. **128**, 1762 (1981).
[24] L. C. Walters and R. E. Grace, J. Phys. Chem. Solids **28**, 239 (1967); **28**, 245 (1967).
[25] A. E. Paladino, J. Am. Ceram. Soc. **48**, 476 (1965).
[26] D. B. Schward and H. U. Anderson, J. Electrochem. Soc. **122**, 707 (1975).
[27] N. G. Eror and U. Balachandran, J. Solid State Chem. **40**, 85 (1981); J. Am. Ceram. Soc. **65**, 426 (1982).
[28] H. Ihrig and D. Hennings, Phys. Rev. B **17**, 4593 (1978).
[29] J. Daniels and K. H. Hardtl, Philips Res. Rep. **31**, 480 (1976).
[30] Z. G. Lu, J. P. Bonnet, J. Reves, and P. Hagennuller, Solid State Ionics **57**, 235 (1992).
[31] E. Iguchi, N. Kubota, T. Nakamori, N. Yamamoto, and K. J. Lee, Phys. Rev. B **43**, 8646 (1991).
[32] E. J. Nakamura, Ferroelectrics **135**, 237 (1992).
[33] E. Parkarsh, D. Kumar, Ch. D. Prasad, and H. S. Tewawri, J. Phys. D **23**, 342 (1990).
[34] M. Maglione and M. Belkaoumi, Phys. Rev. B **45**, 2029 (1992).
[35] G. Burns, Phase Transit. **5**, 261 (1985).
[36] S. A. Long and R. N. Blumenthal, J. Am. Ceram. Soc. **54**, 577 (1971).
[37] R. L. Wild, E. M. Rocker, and J. C. Smith, Phys. Rev. B **8**, 3828 (1973).
[38] R. Waser, T. Baiatu, and K. H. Härdtl, J. Am. Ceram. Soc. **73**, 1645 (1990).